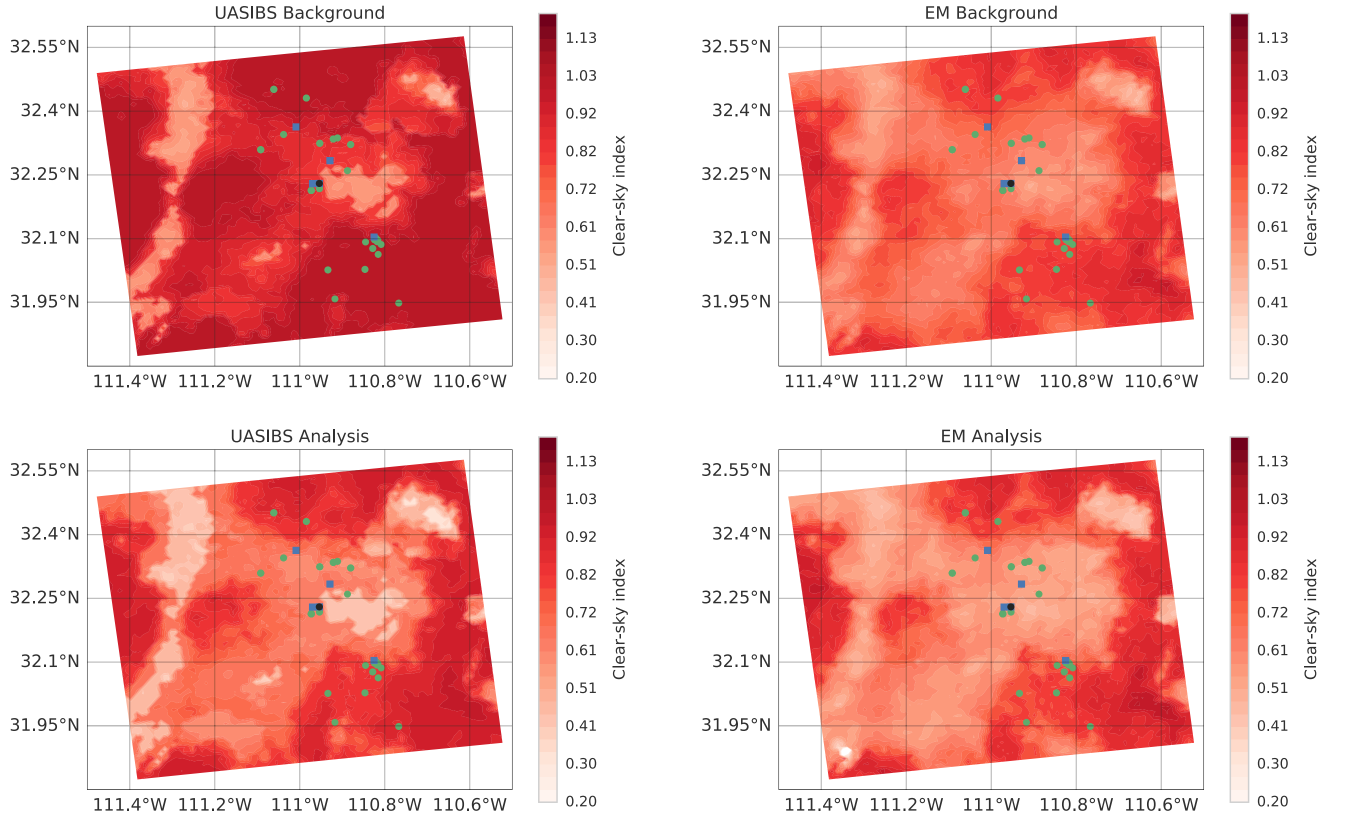

Fig. 2. Example OI results for one image/data taken on 2014-04-19 18:30Z (11:30 AM local time). The top row are the background satellite derived clear-sky index estimates before OI. The lower row are the clear-sky index analysis after performing OI. Satellite derived estimates using the UASIBS model are on the left and those using the EM model are on the right. Lighter shades indicate thicker clouds. The green circles are the sensors used for OI, the blue squares are the sensors used for error analysis, and the black circle in the center is the calibrated NREL MIDC sensor. Comparing the background and analysis, one can see that the thin cloud near the center of the image is made slightly thicker in the analysis.

III. Results

In this section, we present the results of the analysis of roughly 1200 satellite images taken over Tucson, AZ. Both the UASIBS and EM models described above were used to convert the raw satellite images to estimates of GHI at the surface and then used as the background field for the OI algorithm.

Figure 2 shows uncorrected background maps of clear-sky index derived from the UASIBS and EM models and the OI corrected analysis. Notice that in the UASIBS analysis image, the thin clouds in the center of the image are thicker than in the background based on the information of the sensors near the top of the image that measure other parts of the cloud. For the EM model, OI adjusts the cloudy areas to be more cloudy and the clear areas to be more clear. We also see that the analysis images in Fig. 2 are similar suggesting that OI works robustly with different satellite image to GHI models that define the background.

Figure 3 shows an example of the errors of the background and analysis images as compared to sensor observations for a single satellite image/time processed with the UASIBS model. The errors shown are computed from sensors that are *not* used during OI. We see that the absolute error was reduced for all sensors, including the calibrated MIDC sensor and rooftop PV systems. This suggests that the OI correctly propagates information from data to unobserved locations.

We calculated empirical cumulative distribution functions (CDF) for the observations, background, and analysis. Figure 4 shows these CDFs for the UASIBS model. The slope of zero around 0.8 in the CDF of the UASIBS background (red dashed-dotted line) indicates that the UASIBS model does not predict clear-sky indices of 0.8. The analysis (blue dashed line) does predict clear-sky indices in that range and even extends the range over 1.0 to more closely match the observations.

The empirical CDF for the EM model is shown in Fig. 5. We see that the EM model tends to over-predict clouds, but that the OI then removes much of this bias. On the other hand, the figure suggests that the analysis could be improved at smaller clear-sky indices to better match the observations.

For the 1200 images analyzed, root-mean squared errors (RMSE), mean absolute errors (MAE), and mean bias errors (MBE) decreased on average. Error statistics for the EM and UASIBS models in terms of the clear-sky index calculated over all the withheld sensors and for clear, cloudy, and all days are presented in Table I. Error statistics in units of GHI for the calibrated MIDC irradiance sensor are presented in Table II.